Cellular Signalling 27 (2015) 6–14

Contents lists available at ScienceDirect

Cellular Signalling

journal homepage: www.elsevier.com/locate/cellsig

FSH-induced p38-MAPK-mediated dephosphorylation at serine 727 of the signal transducer and activator of transcription 1 decreases *Cyp1b1* expression in mouse granulosa cells

Xue-Hai Du, Xiao-Long Zhou [1], Rui Cao, Peng Xiao, Yun Teng, Cai-Bo Ning, Hong-Lin Liu *

College of Animal Science and Technology, Nanjing Agricultural University, Nanjing 210095, People's Republic of China

ARTICLE INFO

Article history:
Received 31 August 2014
Received in revised form 26 September 2014
Accepted 7 October 2014
Available online 12 October 2014

Keywords:
FSH
Cyp1b1
Granulosa cell
STAT1
p38 MAPK

ABSTRACT

Most mammalian follicles undergo atresia at various stages before ovulation, and granulosa cell apoptosis is a major cause of antral follicular atresia. Estradiol is an essential mitogen for granulosa cell proliferation *in vivo* and inhibition of apoptosis. The estradiol-producing capacity and metabolism levels are important for follicle health, and sufficient estradiol is necessary for follicle development and ovulation. *Cyp1b1*, a member of the cytochrome P450 1 subfamily, is responsible for the metabolism of a wide variety of halogenated and polycyclic aromatic hydrocarbons in diverse tissues. In mouse follicles, Cyp1b1 converts estradiol to 4-hydroxyestradiol. We investigated mouse granulosa cells (MGCs) *in vivo* and *in vitro* and found that *Cyp1b1* played a crucial role in estradiol metabolism in dominant follicles. Follicle-stimulating hormone (FSH) decreased estrogen metabolism by reducing *Cyp1b1* mRNA and protein levels in MGCs. Furthermore, FSH regulated signal transducer and activator of transcription 1 (STAT1), a significant transcription factor of *Cyp1b1*, by mediating the dephosphorylation of STAT1 on serine 727 (Ser^{727}) in MGCs. p38 mitogen-activated protein kinase (MAPK) may be involved in the FSH-induced dephosphorylation of STAT1 on Ser^{727} in MGCs. These results suggested that FSH functions *via* p38 MAPK-induced dephosphorylation at Ser^{727} of STAT1 to downregulate *Cyp1b1* expression and maintain the estradiol levels in mouse dominant follicles.

1. Introduction

In mice, follicular atresia is frequently observed in follicles 250–399 μm in diameter. This size range may be critical for atresia as few follicles in the range 250–399 μm resume meiosis, whereas meiosis is restored in follicles ≥400 μm in diameter, resulting in ovulation [1]. Follicle health depends upon routine biosynthesis and metabolism of estradiol, the predominant sex hormone in females. Sufficient estradiol in the dominant follicle is essential for follicular growth and triggers the surge in preovulatory luteinizing hormone (LH) that promotes ovulation [2,3]. The capacity to produce estradiol is lost in ovarian follicles before atresia [4,5]. The cytochrome P450 superfamily is a large and diverse group of enzymes that catalyze the oxidation of organic substances, such as metabolic intermediates (including lipids and steroidal hormones) and xenobiotic substances (including drugs and other toxic chemicals) [6]. In mammals, 2-hydroxyestradiol (2-OH E2) and 4-hydroxyestradiol (4-OH E2) are two of the main hydroxylated metabolites of estradiol (E2) formed by cytochrome P450 family members *1A1*, *3A*, *1B1*, and *1A2* [7,8]. In adult mice, the cytochrome P450 *1a1* gene is not expressed constitutively, but is highly inducible by foreign compounds acting through the aryl hydrocarbon receptor (AhR) [9]. The catalysis of Cyp1b1 estrogen to 4-OH E2 is considered a dominant metabolic pathway for the formation of catechol estrogen in several extrahepatic tissues [10].

Signal transducer and activator of transcription 1 (STAT1) is activated in response to interferon (IFN)-α, IFN-γ and a large number of ligands [11–13]. The phosphorylation of STAT1 at tyrosine 701 (Tyr^{701}) induces STAT1 dimerization, after which it translocates to the nucleus and acts as a transcription factor (TF) to regulate gene expression [14]. STAT1 protein has two isoforms: STAT1α (91 kDa) and the splice variant STAT1β (84 kDa). STAT1 is also phosphorylated at Ser^{727} in response to IFN-α and other cellular stresses [15–17]. Only STAT1α can be phosphorylated at Ser^{727}, as the site is deleted in STAT1β. Serine phosphorylation of STAT proteins is required for maximal tyrosine phosphorylation, DNA binding, transcriptional activity and regulation of gene transcription. Inappropriate activation of STAT1 occurs in many tumors [18].

Follicle-stimulating hormone (FSH) promotes the synthesis of estrogen. However, it is unclear whether FSH is involved in estrogen

Abbreviations: MGCs, mouse granulosa cells; 4-OH E2, 4-hydroxyestradiol; STAT1/3, signal transducer and activator of transcription 1/3; TF, transcription factor; p-Ser^{727} STAT1, phosphorylation of STAT1 on Ser^{727}; p-Tyr^{701} STAT1, phosphorylation of STAT1 on Tyr^{701}; BS 1/2, binding site 1/2; Cyp1b1, cytochrome P450, family 1, subfamily b, polypeptide 1; p38 MAPK, p38 mitogen-activated protein kinase; IFN-α, interferon-α.

* Corresponding author. Tel./fax: +86 25 84395106.
E-mail address: liuhonglin@njau.edu.cn (H.-L. Liu).

[1] This author contributes equally to the first author.

http://dx.doi.org/10.1016/j.cellsig.2014.10.002
0898-6568/

metabolism. To examine the relationship between FSH and estrogen metabolism, we investigated the mechanisms of FSH regulation relevant to the estradiol metabolism gene *Cyp1b1* in mouse granuloma cells (MGCs). FSH stimulation induced dephosphorylation of STAT1 on Ser^{727} in MGCs; this effect was blocked by a p38 mitogen-activated protein kinase (MAPK) inhibitor in response to FSH stimulation. Our study showed that STAT1 is important for FSH regulation of the Cyp1b1 gene expression and estradiol metabolism in mouse dominant follicles.

2. Materials and methods

2.1. Animals

Female imprinting control region (ICR) mice were obtained from the Qing Long Shan Co., Animal Breeding Center (Nanjing, China). FSH (Ningbo Second Hormone Factory, Ningbo, China) was administered intraperitoneally to 4-week-old female mice four times (10, 10, 5, and 5 IU) at 12-h intervals. No human chorionic gonadotropin (HCG) was injected in mice after FSH stimulation, and several dominant follicles (250–399 μm) that did not progress to ovulation were collected for analysis. Mice were sacrificed by cervical dislocation, and MGCs were collected from the dominant ovarian follicles at 48 h after the first FSH injection. At 66 h, additional FSH (10 IU) and PBS injections were administered to the mice, and MSGs were collected at 72 h, hereafter called 72–66 h (mice injected with FSH at 66 h) and 72 h (mice injected with PBS), respectively. All animal experiments were performed according to the guidelines of the regional Animal Ethics Committee.

2.2. Cell culture

Intact mice were injected intraperitoneally with FSH (10, 10, 5, and 5 IU) and sacrificed 48 h later. MGCs were harvested from the ovarian dominant follicles. Cells were cultured in Dulbecco's Modified Eagle's medium (DMEM) F12 containing 10% (v/v) fetal calf serum (FCS) with and without FSH (F4021; Sigma-Aldrich, St. Louis, MO, USA), LY294002 (S1737; Beyotime), IFN-α (PMC4016; Invitrogen, Carlsbad, CA, USA), and SB203580 (S1863; Beyotime), and incubated at 37 °C with 5% CO_2.

2.3. Real-time quantitative polymerase chain reaction (PCR) analysis

Relevant primers for *Cyp1b1*, *STAT1*, *NF-E2*, *Pou2f1*, *Arnt*, *Cyp3a*, *Cyp1a2*, and *β-Actin* were designed using the Primer 5 software, and *GAPDH* was used as an internal control (Table 1). In this study, all PCR products produced single bright bands of the expected sizes, and the melting-curve analysis of each band showed only one peak. Total RNA was extracted from the granulosa cells using TRIzol® (Invitrogen) according to the manufacturer's instructions. Reverse transcription of total RNA was performed using a RevertAid™ RT reagent kit (EP0441; Fermentas, Germany) in a 25-μl reaction mixture according to the manufacturer's instructions.

2.4. Annexin V-fluorescein isothiocyanate (FITC) apoptosis assay

Cultured MGCs were treated with 4-OH E2 for 24 h. Media were collected from the cultured cells. After washing, the MGCs were digested with pancreatin without EDTA for 5 min. The collected media were added, and the samples were then centrifuged at 1000 *g* for 5 min. The supernatant was discarded and the pellet was resuspended in PBS for cell counting. After two washes with PBS, 50,000–100,000 cells were centrifuged at 1000 *g* for 5 min and the supernatant was discarded. Annexin V-FITC buffer (195 μl) and annexin V-FITC dye (5 μl) were added to the tubes, which were then rocked gently at 25 °C for 10 min before centrifugation at 1000 *g* for 5 min. The supernatant was discarded, and 190-μl PI buffer and 10-μl PI dye were added. Samples were rocked uniformly before being placed on ice in lucifugal conditions in preparation for flow cytometry analysis.

Table 1
Primers for real-time quantitative PCR.

Gene name	Primer sequence (5′ → 3′)	Size (bp)	Tm/(°C)
Cyp1b1 (NM_009994.1)	F: CACTATTACGGACATCTTCGG R: AGGTTGGGCTGGTCACTC	168	56
STAT1 (NM_001205313.1)	F: CTCATTGTCACCGAAGAAC R: CTGCCAACTCAACACCTC	264	58
Pou2f1 (NM_011137.3)	F: CAGTGAAGAGTCGGGAGAT R: TGTATGGGCTGAGACAGG	294	56
NF-E2 (NM_008685.2)	F: TTGTGAAGAGTGCGTGTCCG R: CCCGCAGGTGCTGGTTTA	160	55
Arnt (NM_001037737.2)	F: CGGTAAGGTGCCTAATCT R: CTGATGTCATTTCTGGGTT	142	58
Cyp3a (NM_007818.3)	F: TTTTCTGTCTTCACAAACCGG R: TAACAGGCTTGCCTTTCTTTG	200	55
Cyp1a2 (NM_009993.3)	F: TGCCATCTTCTGTTTAGTGTT R: CCCTTGAAGTCATCTCCCT	267	56
β-Actin (NM_007393.3)	F: GCTGTCCCTGTATGCCTCT R: GTCTTTACGGATGTCAACG	460	60.8
GAPDH (NM_008084.2)	F: ATGGTGAAGGTCGGTGTGAACG R: CTCGCTCCTGGAAGATGGTGATG	235	58
Cyp1b1 BS 1	F: CTCGGCGTGTCAGGTGTCGT R: AGGAGGAGGCGGCTCTGTAC	182	58
Cyp1b1 BS 2	F: CACGCTTCATCGCAGGTC R: GCCTAACGGTTCCCAGAA	163	55
Cyp1b1 Exon 3	F: GGAAGAAGGGTACAAGCC R: GCCGCACTGATCTGAAGT	160	55

2.5. Plasmids

Full-length mouse STAT1 cDNA from adult ovaries was inserted into the *BamH*I and *Xho*I sites of the pcDNA3.1 (+) vector (Invitrogen); the resulting expression vector was denoted as pcDNA3.1-STAT1. A mouse *Cyp1b1* luciferase reporter plasmid was constructed by inserting the promoter regions from −1208 to +818 into the *Kpn*I and *Sma*I sites of the pGL3-Basic vector (Promega, Madison, WI). The two predicted binding sites of STAT1 on *Cyp1b1* were BS 1 (from −908 to −900) and BS 2 (from +486 to +494). Mutant versions of the *Cyp1b1* luciferase reporter with mutations in the BS 1 (mutant 1), BS 2 (mutant 2), or both BS 1 and BS 2 (mutant 3) were generated using site-directed mutagenesis with the Vazyme Mut Express™ Fast Mutagenesis Kit. The vectors were denoted as pGL3-*Cyp1b1*-WT, pGL3-*Cyp1b1*-mutant 1, pGL3-*Cyp1b1*-mutant 2 and pGL3-*Cyp1b1*-mutant 3 respectively. The primers used to construct plasmids are listed in Table 2.

2.6. Luciferase reporter assays

NIH 3T3 cells were seeded in 12-well plates 24 h before transfection. On the day of transfection, each well was cotransfected with 0.75 μg of the pcDNA3.1-STAT1 plasmid, 0.75 μg of the pGL3 vector and 50 ng of the pRL-TK vector (Promega) using Lipofectamine 2000 (Invitrogen). The luciferase assay was performed 48 h after transfection as described previously [19] using the dual-luciferase reporter assay system (Promega).

2.7. Enzyme-linked immunosorbent assay (ELISA) analysis

After dominant ovarian follicles were punctured (20 punctured follicles from each mouse, $n = 7$ mice/group), 4-OH E2 and E2 were extracted using 50-μl 20% DMSO. The concentrations of 4-OH E2 and E2 were performed according to the manufacturer's protocol using the 4-OH E2 ELISA kit (E-20620, R&D systems subpackage) and E2 ELISA kit (E-20380, R&D systems subpackage). Because the follicle sizes

Table 2
Primers for plasmid construction.

Gene name	Primer sequence (5′ → 3′)	Size (bp)	Tm/(°C)
STAT1	F:GGGGTACCTTGCATTGACCATAAACAAGAGC	2026	66
(NM_001205313.1)	R:TCCCCCGGGAGGACGGAGAAGAGTAGCAGAAG		
Cyp1b1	F:GGGATCCCCAGTAAGTCTACGTGGGAACG	2340	66
(NM_009994.1)	R:CCCTCGAGGAAGGAATCACAGATGGGAAAA		
Cyp1b1-BS1-Mutant	F:AGCCGAC***GATGT***A***TTG***GCGGCGCACGCAAGGCACAGCTCCGCAC		
	R:CGCCGC***CAA***T***ACATC***GTCGGCTCCAGTCATCTCCCTGGGCGCT		
Cyp1b1-BS2-Mutant	F:TCGGAAT***GACTTAGC***CCGTTAGGCAGCTGGGGATTTGGAAGCCGAT		
	R:CCTAACGG***GCTAAGTC***ATTCCGACACAATGCCGGTGGGTGGCAG		

differed, the concentrations of 4-OH E2 and E2 did not accurately reflect estradiol metabolism. Therefore, we evaluated estradiol metabolism by means of the 4-OH E2/E2 ratio.

2.8. Western blot analysis

MGCs were lysed in RIPA lysis buffer (P0013B, Beyotime) with 1 mM PMSF (ST506, Beyotime) to prepare total proteins. The concentration of protein samples was determined using the BCA method (Pierce, Rockford, IL, USA). For each sample, 10-μg total protein was loaded onto a 12% SDS-PAGE gel and processed at 60 V for 3–4 h before transferring to a nitrocellulose membrane (Pall, Port Washington, NY, USA) using an electroblotting method. The sample was then processed at 100 V for 90 min. After incubation in blocking buffer [TBST with 1% (w/v) BSA (A7030; Sigma)] for 1 h, the membranes were incubated at 4 °C for 12 h with an anti-STAT1 (9172; Cell Signaling Technology, Beverly, MA, USA), anti-p-Ser^{727} STAT1 (9177; Cell Signaling Technology), anti-p-Tyr^{701} STAT1 (9167; Cell Signaling Technology), or anti-Cyp1b1 (SC-32882; Santa Cruz Biotechnology, Santa Cruz, CA, USA) antibody. After washing, the membranes were incubated with an HRP-conjugated goat anti-rabbit IgG secondary antibody (SC-2030; Santa Cruz Biotechnology) for 1 h at room temperature and then washed. The membranes were visualized with an ECL Western blot detection kit (NC15080; Thermo Fisher Scientific, Waltham, MA, USA). α-Tubulin (T5168; Sigma) and STAT1 protein levels served as internal controls. The chemiluminescence of each protein band was quantified using the ImageJ software, and protein levels were normalized to those of α-tubulin or STAT1.

2.9. Immunofluorescence

MGCs were grown on coverslips. After treatment, the cells were fixed with 4% paraformaldehyde. Coverslips were rinsed three times for 5 min each in PBS, incubated in 100% methanol for 10 min at −20 °C, and then rinsed again in PBS for 5 min. After incubation in blocking buffer for 2 h (PBS with 0.3% Triton X-100 and 1% BSA), the coverslips were incubated with an anti-p-Ser^{727} STAT1 antibody (9177; Cell Signal Technology) for 12 h at 4 °C. The coverslips were then incubated with a goat anti-rabbit IgG 488 (CA11008s; Invitrogen) conjugated to Alexa Fluor 488 (green) for 50 min in darkness. After staining the cell nuclei with DAPI for 15 min, fluorescent images were taken using a confocal laser scanning microscope (Carl Zeiss, Germany).

2.10. Chromatin immunoprecipitation (CHIP) assay

Formaldehyde (1% final concentration) was added directly to the media containing the MGCs. Fixation proceeded at room temperature for 10 min and was stopped by the addition of glycine to a final concentration of 0.125 M. The MGCs were collected by centrifugation and rinsed three times in cold PBS with 1 mM PMSF. The cell pellets were resuspended in lysis buffer [50 mM Tris (pH 7.4), 150 mM NaCl, 1% Triton X-100, 1% sodium deoxycholate, 1% SDS, sodium orthovanadate, sodium fluoride, EDTA, 100 ng leupeptin and aprotinin/ml, and 1 mM PMSF] for 30 min on ice, and vortexed for 15 s every 5 min. After lysis, the samples were sonicated on ice (MPI Ultrasonics, Switzerland) at setting 5 for six 10-s pulses to create an average length of 400–800 bp. Immunoprecipitation (IP) and DNA recovery were performed using a Pierce agarose CHIP kit (26156; Thermo Fisher Scientific). Anti-p-Ser^{727} STAT1 antibody (9177; Cell Signal Technology) was used for IP. After IP elution and DNA recovery, DNA in the IP samples was quantified by real-time PCR and normalized to input DNA control samples. Primer information is provided in Table 1.

2.11. Statistical analyses

Results are presented as means ± SEM. Statistical analysis was performed using the SPSS 16.0 software (SPSS, Inc.). Comparisons of two means were performed with Student's independent *t*-tests. Comparisons of three or more means were performed by one-way analysis of variance. The mean differences were considered significant at $P < 0.05$.

3. Results

3.1. Cyp1b1 mRNA and protein levels are reduced by FSH in MGCs

In mammals, estradiol is converted by Cyp1a1, Cyp3a, Cyp1b1, and Cyp1a2 to 2-OH E2 and 4-OH E2 [8]. However, the cytochrome P450 *1a1* gene is not constitutively expressed in female mice [9]. Low *Cyp1a2* and *Cyp3a* mRNA levels were found in granulosa cells compared with those in liver cells, and only the *Cyp1b1* gene showed continuous expression in the mouse ovary [20] (Fig. 1). Thus, the *Cyp1b1* gene is important for estradiol metabolism in the granulosa cells of mouse follicles.

After FSH treatment, granulosa cells were extracted directly from the dominant follicles at 48 and 72 h. Total RNA was extracted and RT-PCR

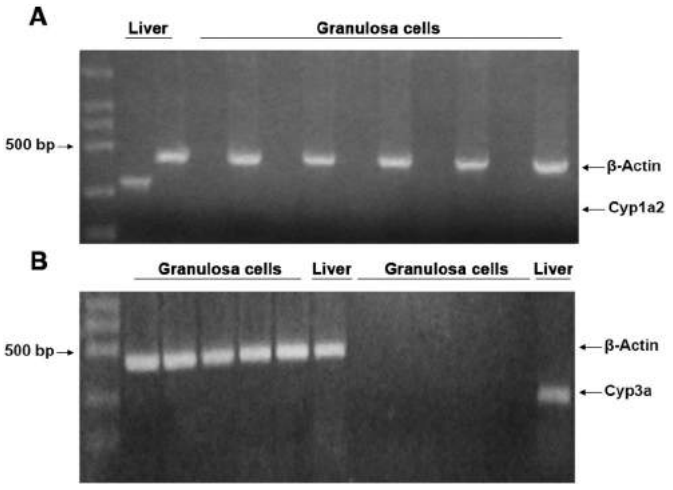

Fig. 1. Expression of estradiol metabolism-relevant genes in mouse dominant follicles. (A, B) Mouse granulosa cell and liver cell cDNA amplified by reverse transcription polymerase chain reaction (RT-PCR; 40 cycles) and visualized on an agarose gel.

was performed. A significant decrease ($P < 0.05$) in the *Cyp1b1* mRNA level was observed in mice injected with FSH at 66 h (72–66 h group), whereas the mRNA levels were higher in the mice injected with PBS at 66 h (72 h group) *in vivo* (Fig. 2A).

Granulosa cells cultured *in vitro* were treated with FSH (10, 50, 100, 150 ng/ml). We found that 100 ng/ml FSH induced significant downregulation of *Cyp1b1* mRNA levels (Fig. 2B). Moreover, Cyp1b1 protein levels were also significantly downregulated by FSH (Fig. 2C–D).

3.2. FSH reduced the estrogen metabolism level by downregulating Cyp1b1 expression

As estradiol is converted mainly to 4-OH E2 by Cyp1b1, inhibiting Cyp1b1 expression was expected to reduce 4-OH E2 and maintain E2 levels in mouse follicles. We performed ELISA to assess 4-OH E2 and E2 levels in delayed ovulation dominant follicles. Compared with the 48-h groups, the 4-OH E2/E2 ratio was significantly increased in the 72-h groups, and was reduced significantly by the addition of 10 IU FSH at 66 h (72–66-h group) (Fig. 3). These results indicated that FSH reduced the estrogen metabolism level by downregulating Cyp1b1 expression.

In vitro, cultured MGCs were treated with various doses of 4-OH E2 for 24 h, and the apoptosis rate was determined by flow cytometry analysis of annexin V-FITC staining. We found that 10 μM 4-OH E2 significantly induced granulosa cell apoptosis (Fig. 4). Thus, FSH inhibition of estrogen metabolism maintained estradiol levels and reduced 4-OH E2 accumulation, which was harmful to MGCs in mouse dominant follicles.

3.3. Involvement of STAT1 in FSH-mediated control of Cyp1b1 expression

To determine the mechanism by which FSH downregulated *Cyp1b1* expression, we analyzed the TFs predicted to regulate *Cyp1b1*; *e.g.*, STAT1, Pou2f1, NF-E2, and Arnt. TF mRNA levels were assayed by RT-PCR, and the distance correlation analysis between *Cyp1b1* and TFs was performed using SPSS ver. 16.0. *STAT1* mRNA levels were most similar to those of *Cyp1b1* (Fig. 5A and B).

We next performed CHIP assays to further assess the relationship between STAT1 and *Cyp1b1*. As shown in Fig. 5C, the STAT1-binding sites on *Cyp1b1* were predicted using www.cbrc.jp/research/db/TFSEARCH.html. Granulosa cells from three mice were combined to form one sample group. After DNA recovery, three rounds of RT-PCR were performed on the samples. STAT1 BS 1 and 2 binding to *Cyp1b1* was decreased significantly in the 72–66-h group compared to the levels in the 72-h group after FSH stimulation (Fig. 5D). These results suggested that STAT1 is involved in FSH-mediated control of *Cyp1b1* expression.

Groups	48h	72-66h	72h
Number of Ovary follicles	140	140	140
Concentrations ratio of 4OH-E2/E2	11.55±0.70 a	8.96±0.99 b	14.34±1.05 c
95% Confidence Interval for Mean	9.60-13.50	6.55-11.38	11.77-16.92

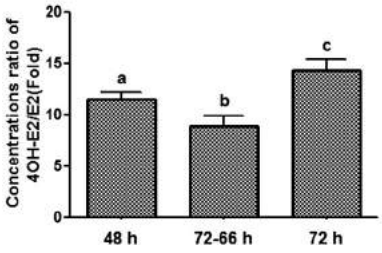

Fig. 3. FSH decreased the estrogen metabolism level in delayed-ovulation follicles. Mouse follicular fluids were extracted directly from the dominant follicles at 48 and 72 h after FSH treatment. Additional FSH (10 IU) or PBS was administered to injected mice at 66 h after FSH treatment in the 72–66-h and 72-h groups, respectively. Concentrations of 4-hydroxyestradiol (4-OH E2) and estradiol (E2) in mouse delayed-ovulation follicles were detected by enzyme-linked immunosorbent assay (ELISA). The 4-OH E2 to E2 ratio was measured to determine the 4-OH E2 content in the follicle ($n = 140$/group). Graphs show means ± SEM. Letters denote significant ($P < 0.05$) differences between values.

3.4. STAT1 as a TF regulated the expression of Cyp1b1

To determine whether STAT1 functions as a TF to regulate *Cyp1b1* expression, we generated the pcDNA3.1-STAT1 ultra-expression plasmid,

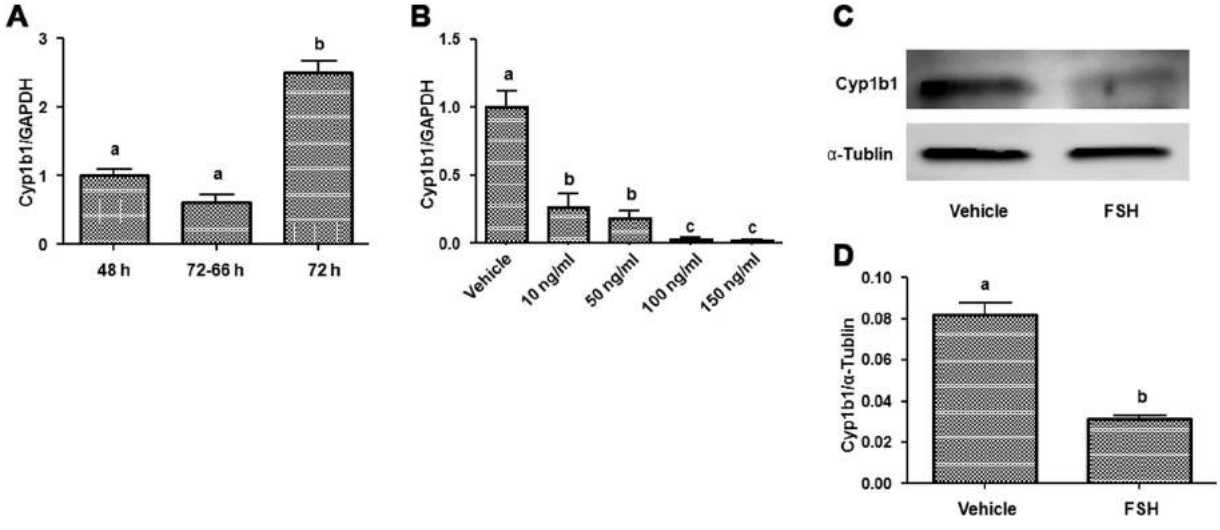

Fig. 2. Regulation of *Cyp1b1* mRNA and protein levels in mouse granulosa cells (MGCs) by follicle-stimulating hormone (FSH). (A) MGCs were collected at 48 and 72 h after FSH treatment. Additional FSH (10 IU) or PBS was administered to injected mice at 66 h after FSH treatment in the following groups: 72–66 h (FSH injected at 66 h) and 72 h (PBS injected at 66 h). The effect of FSH on *Cyp1b1* mRNA levels was measured in granulosa cells of mouse dominant follicles *in vivo* ($n = 7$/group). The mean value in the 48-h group was set as 1. (B) MGCs were cultured with the indicated amounts of FSH for 24 h. The effects of FSH on *Cyp1b1* mRNA levels were analyzed by quantitative reverse transcription-polymerase chain reaction (qRT-PCR) ($n = 3$/group). The mean value in the vehicle group was set as 1. (C) FSH (100 ng/ml) suppressed Cyp1b1 protein levels in cultured MGCs. MGCs were cultured with or without FSH (100 ng/ml) for 24 h. Whole-cell lysates were harvested from the treatment groups as indicated. Immunoblotting was performed to detect Cyp1b1 expression. α-Tubulin served as an internal control ($n = 3$/group). (D) Quantification of relative Cyp1b1 protein levels by gradation analyses. The ImageJ software was used to analyze the gradation of each band represented in panel C, and the relative expression levels were normalized to that of α-tubulin. Graphs show means ± SEM. Letters denote significant ($P < 0.05$) differences between values.

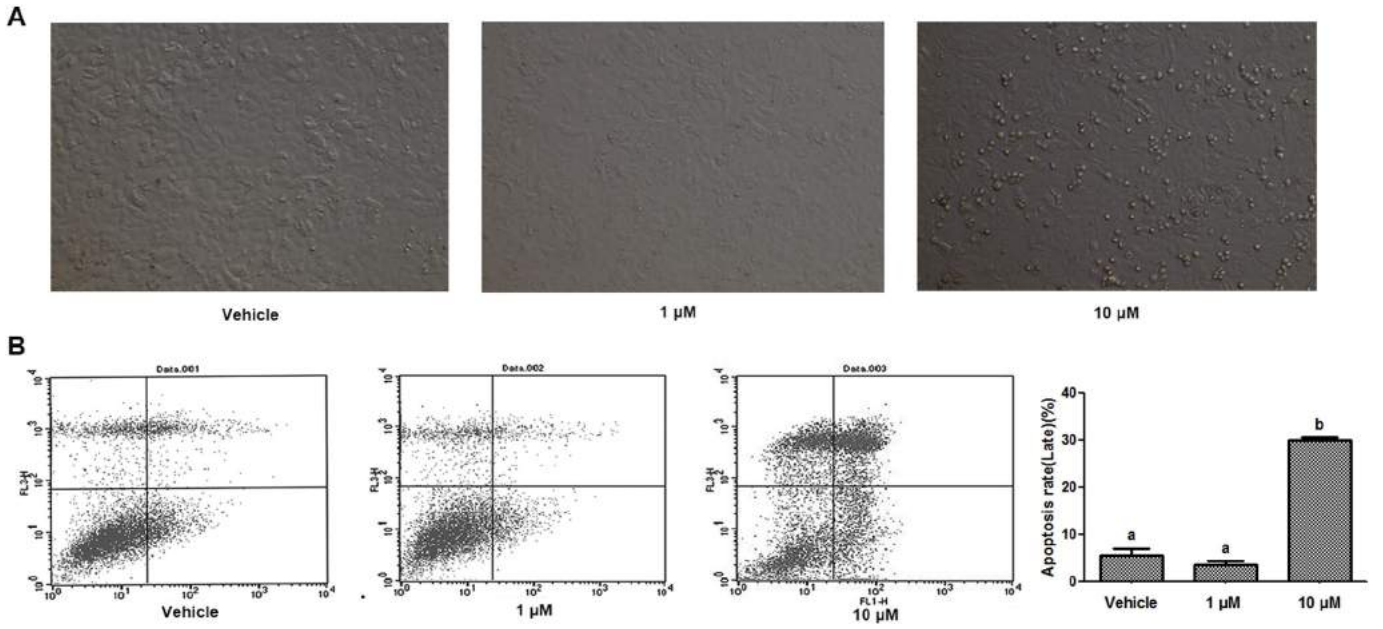

Fig. 4. 4-OH E2 stress-induced apoptosis of MGCs *in vitro*. (A) Phase-contrast images of MGCs treated with the indicated doses of 4-OH E2. (B) Histograms and quantitative analyses by flow cytometry of annexin V-fluorescein isothiocyanate (FITC) staining in MGCs treated with the indicated doses of 4-OH E2 ($n = 3$). Graphs show means ± SEM. Letters denote significant ($P < 0.05$) differences between values.

pGL3-*Cyp1b1*(−1208/+818) luciferase reporter plasmid, and pGL3-*Cyp1b1*(−1208/+818) luciferase reporter plasmid with mutations in BS 1 and BS 2 (Fig. 7A). These mutations aimed to block STAT1 binding to BS 1 (mutant 1), BS 2 (mutant 2), or both BS 1 and BS 2 (mutant 3). *In vitro*, cultured granulosa cells were collected at 48 and 72 h after transfection with 4-μg pcDNA3.1-STAT1 or pcDNA3.1 in six-well plates. Total RNA was extracted and analyzed using RT-PCR, and total proteins were extracted for Western blot analysis. Compared with the control groups, the overexpression of STAT1 significantly increased *Cyp1b1* mRNA and protein levels (Fig. 6). Thus, the expression of *Cyp1b1* was regulated by STAT1.

To determine the importance of BS 1 and BS 2 in the *Cyp1b1* promoter, pGL3-*Cyp1b1*-WT and pGL3-*Cyp1b1*-mutants were cotransfected with pcDNA3.1-STAT1 and pRL-TK in NIH 3T3 cells. The dual-luciferase reporter assay showed that BS 1 and BS 2 were functional, and that mutated BS 2 decreased the transcriptional activity of *Cyp1b1* to the same level as mutated BS 1. Both the BS 1 and BS 2 mutations further decreased the transcriptional activity of *Cyp1b1* (Fig. 7B). These results suggested that BS 1 and BS 2 played equally important roles in STAT1 regulation of *Cyp1b1* transcription activity. Therefore, STAT1 functions as a TF for, and regulates the expression of, *Cyp1b1*.

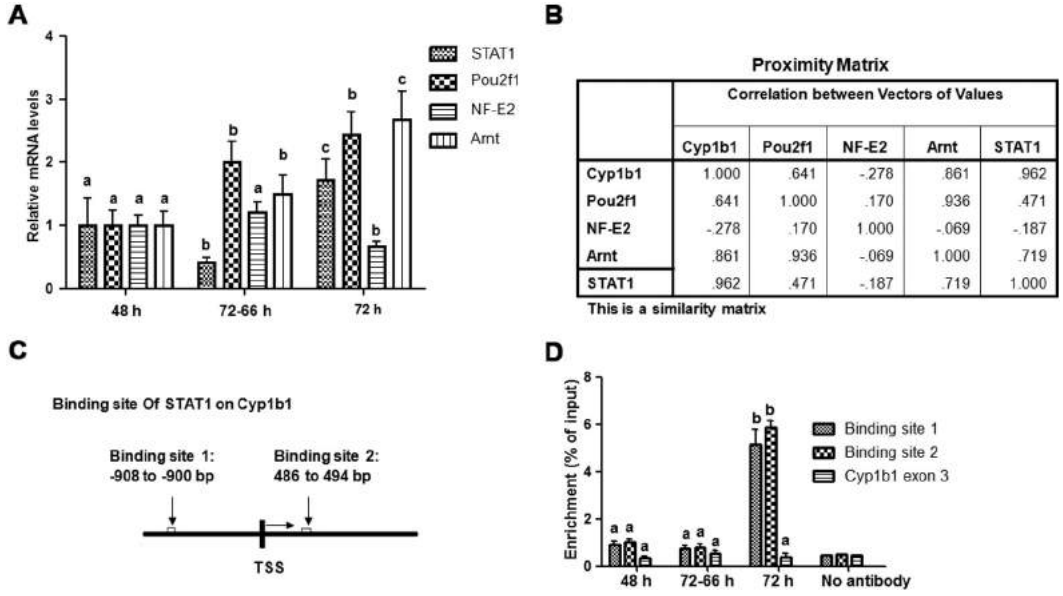

Fig. 5. Effect of FSH on transcription factors (TFs) of *Cyp1b1* in MGCs of dominant follicles *in vivo*. (A) The effects of FSH on *Cyp1b1* TFs were analyzed by qRT-PCR. The mean value in the 48-h group was set as 1 ($n = 7$/group). Graphs show means ± SEM. Letters denote significant ($P < 0.05$) differences between values. (B) Correlations between TFs and *Cyp1b1* were determined by SPSS 16.0 using the correlate-distance program. (C) The predicted binding sites of STAT1 to *Cyp1b1*. (D) Whole granulosa cell lysates were harvested from the treatment groups as indicated. Following immunoprecipitation with an anti-signal transducer and activator of transcription 1 (STAT1) antibody, enrichment of the STAT1-containing DNA sequence was quantified by real-time PCR. Relative amounts of the STAT1-containing DNA sequence compared to the *Cyp1b1* input in each group were calculated ($n = 3$/group). Graphs show means ± SEM. Letters denote significant ($P < 0.05$) differences between values.

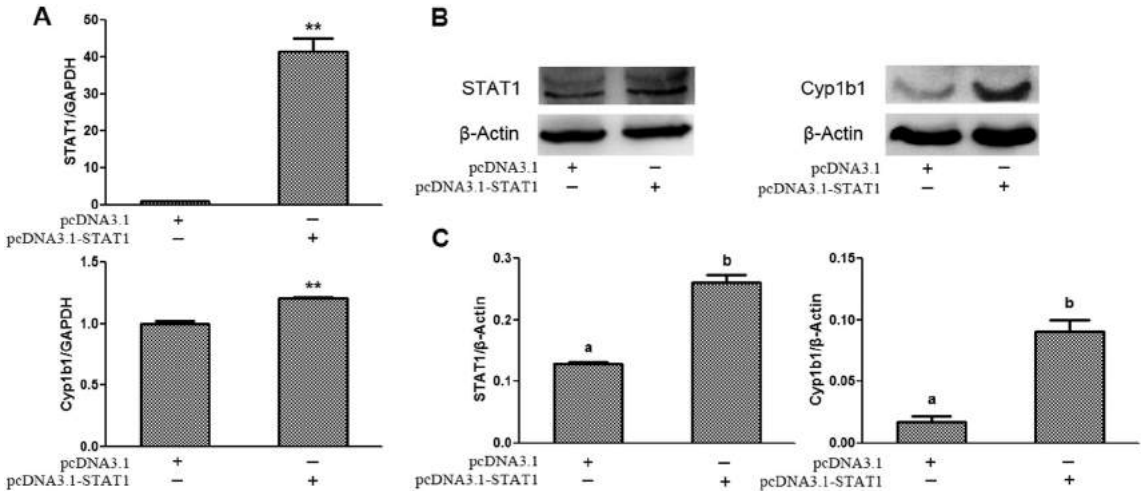

Fig. 6. STAT1 regulation of *Cyp1b1* mRNA and protein levels in MGCs. (A) Cultured MGCs were collected at 48 h after transfection with pcDNA3.1-STAT1 or pcDNA3.1. The mRNA levels of *STAT1* and *Cyp1b1* were analyzed by qRT-PCR ($n = 3$/group). The mean value in the transfection of pcDNA3.1 group was set as 1. (B) Whole-cell lysates were harvested from cultured MGCs at 72 h after transfection with pcDNA3.1-STAT1 or pcDNA3.1. Immunoblotting was performed to detect STAT1 and Cyp1b1 levels. β-Actin served as an internal control ($n = 3$/group). (C) Quantification of relative STAT1 and Cyp1b1 protein levels by gradation analyses. The ImageJ software was used to analyze the gradation of each band represented in panel B, and the relative expression levels were normalized to that of β-Actin. Graphs show means ± SEM. Letters denote significant ($P < 0.05$) differences between values. $^{**}P < 0.01$.

3.5. Reduction of the phosphorylation level of STAT1 on Ser^{727} by FSH

To determine the effect of FSH on the enrichment of STAT1 in the *Cyp1b1* promoter region, mice were injected with FSH four times every 12 h to induce follicle growth. MGCs were collected at 48 and 72 h after the first FSH injection. MGCs were collected and total proteins were extracted for Western blot analysis. STAT1 protein levels showed no significant differences among the three groups. No phosphorylation of STAT1 on Tyr^{701} was detected in MGCs of dominant follicles; however, the phosphorylation level of STAT1 on Ser^{727} was altered. The addition of FSH (10 IU) at 66 h (72–66 h) significantly decreased the level of STAT1 phosphorylation on Ser^{727} compared with that at 72 h (PBS at 66 h) (Fig. 8A–C), similar to the effect of FSH on *Cyp1b1* expression. This result suggested that FSH affected the enrichment of STAT1 in the *Cyp1b1* promoter region by decreasing the phosphorylation level of STAT1 on Ser^{727}.

FSH (100 ng/ml) was added to cultured MGCs, and cells were collected at 6, 12, and 24 h thereafter. The phosphorylation levels of STAT1 on Ser^{727} were detected by immunofluorescence, and found to be significantly decreased at 12 and 24 h after FSH stimulation (Fig. 9A and B).

Western blot analysis of STAT1 protein levels showed no significant change after FSH treatment, but the phosphorylation level of STAT1 on Ser^{727} was decreased significantly at 12 and 24 h after FSH treatment. No phosphorylation of STAT1 on Tyr^{701} was detected in any of the *in vitro* groups (Fig. 9C and D). To confirm the negative effects of STAT1 phosphorylation on Tyr^{701} in cultured MGCs, IFN-α (500 U/ml) was added to the culture medium. After 30 min, proteins were collected; additionally, proteins were collected from the other two groups at 24 h after treatment. The IFN-α-treated group showed a more intense band of p-Tyr^{701} STAT1 compared with the other two groups (Fig. 9E). These results indicated that FSH induced dephosphorylation of STAT1 on Ser^{727} but not on Tyr^{701} to downregulate *Cyp1b1* expression.

3.6. FSH via p38 MAPK induced dephosphorylation of STAT1 on Ser^{727}

The PI3K/AKT inhibitor LY-294002 (5 μM) and p38 MAPK inhibitor SB-203580 (10 μM) were added to cultured MGCs to determine the

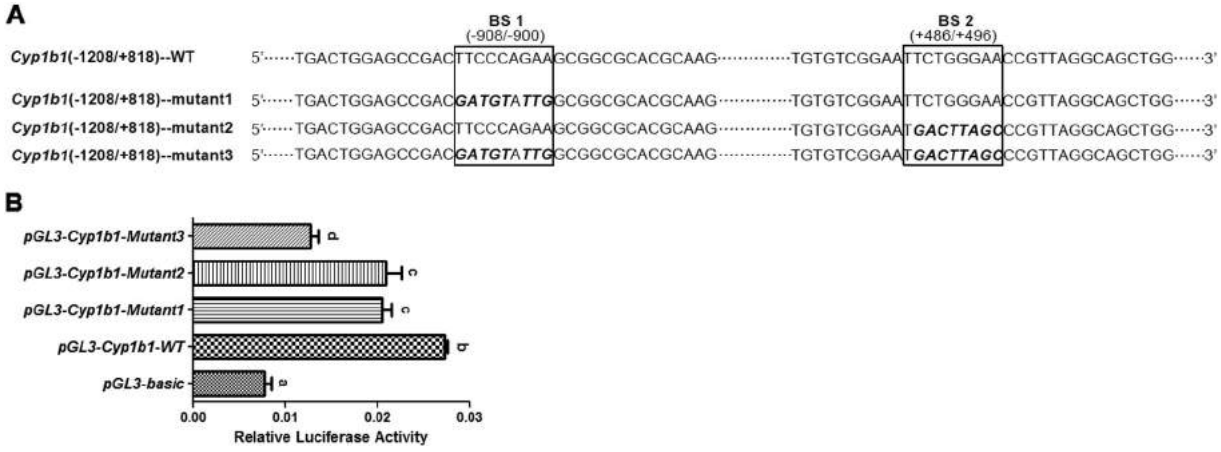

Fig. 7. The effect of STAT1 on *Cyp1b1* was mediated *via* BS 1 and BS 2 within the *Cyp1b1* promoter region. (A) Partial DNA sequences of the mouse *Cyp1b1* promoter region and mutations in the putative BS 1 (mutant 1), BS 2 (mutant 2), or both the BS 1 and BS 2 (mutant 3). (B) Functional importance of the putative binding sites was evaluated by mutating the indicated nucleotides within the context of the pGL3-luciferase reporter plasmid and comparing the activities of these mutant reporters to that of the wild type in NIH 3T3 cells cotransfected with pcDNA3.1-STAT1 and pRL-TK. Luciferase activity was measured as described above. Each panel shows a representative of triplicate experiments. Graphs show means ± SEM. Letters denote significant ($P < 0.05$) differences between values.

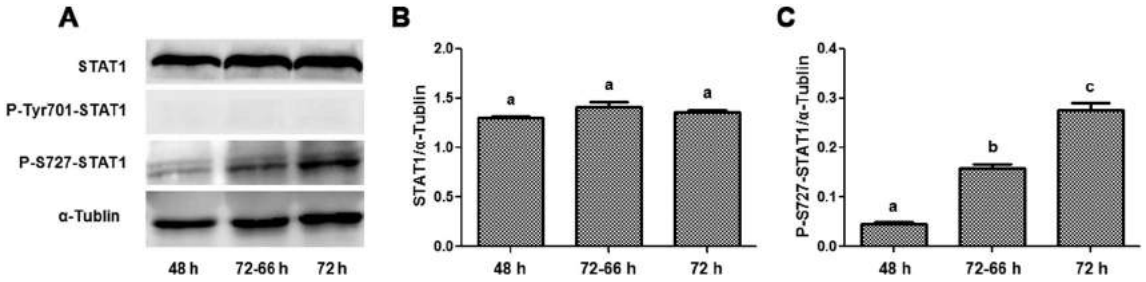

Fig. 8. Effect of FSH on TF STAT1 in MGCs of dominant follicles *in vivo*. (A) Whole-cell lysates were harvested from different treatment groups as indicated. Immunoblotting was performed to detect p-Ser^{727}, p-Tyr^{701}, and STAT1 levels, and STAT1 expression. (B, C) Quantification of relative STAT1 and p-Ser^{727} STAT1 protein levels by gradation analyses. The ImageJ software was used to analyze the gradation of each band represented in panel A, and the relative expression levels were normalized to that of α-tubulin. Graphs show means ± SEM ($n = 3$/group). Letters denote significant ($P < 0.05$) differences between values.

pathway of p-Ser^{727} STAT1 dephosphorylation. As shown in Fig. 10A, SB-203580 inhibited FSH-mediated dephosphorylation of p-Ser^{727} STAT1, whereas LY-294002 did not. Western blot analysis showed that the p38 MAPK inhibitor blocked FSH-mediated dephosphorylation of p-Ser^{727} STAT1 (Fig. 10B–C). These results revealed that p38 MAPK was involved in the dephosphorylation of STAT1 on Ser^{727} induced by FSH.

4. Discussion

In this study, we revealed an unexpected relationship between FSH and estrogen metabolism. We found that FSH inhibited estrogen metabolism, and *Cyp1b1* was important for estradiol metabolism in the granulosa cells of mouse follicles. We investigated the mechanisms of FSH inhibition of estrogen metabolism in MGCs and found that FSH could downregulate *Cyp1b1* expression in MGCs to maintain estradiol levels in dominant follicles. Estradiol is a mitogen for the proliferation of granulosa cells *in vivo*, and is synthesized through LH stimulation of theca cells to synthesize androgens (androstenedione and testosterone), which are substrates for FSH-induced aromatization to produce estradiol [21]. In addition, estrogen facilitates granulosa cell differentiation by increasing LH receptor expression [22], increasing the number of gap junctions between granulosa cells [23], and inhibiting granulosa cell apoptosis [24]. Cultured granulosa cells (but not theca cells) are the prime sites of follicular estrogen production [25]. A sufficient concentration of estradiol is critical for maintaining follicle health until ovulation. Some studies have suggested that estrogen may suppress the activity of Ca^{2+}/Mg^{2+}-dependent endonucleases [26].

Catechol estrogens are hydroxylated metabolites of estradiol that may be involved in the cytotoxicity and genotoxicity generated by Cyp1b1 [27]. Catechol estrogens are catalyzed by peroxidase to produce semiquinone radicals [28]. Semiquinone radicals are readily oxidized by molecular oxygen to yield quinine, along with superoxide anions [29, 30]. High reactive oxygen species levels are harmful to MGCs as they can cause DNA damage and cell death [31]. Reactive quinone can form a conjugate with GSH and deplete cellular thiol, rendering cells vulnerable to apoptosis [32]. Estradiol can be transformed into 4-OH E2 by Cyp1b1 in mammalian follicles, and a high 4-OH E2 concentration induced apoptosis and death in MGCs *in vitro* (Fig. 4). FSH-mediated downregulation of *Cyp1b1* expression may reduce the synthesis of catechol estrogens and protect cells from damage.

FSH inhibited *Cyp1b1* expression in MGCs; however, the regulatory mechanism is unclear and requires further study. AhR, a member of the basic helix–loop–helix TF family, is a cytosolic TF that is normally inactive. *AhR* is activated by the binding of several classes of structurally diverse aromatic compounds and environmental pollutants, such as

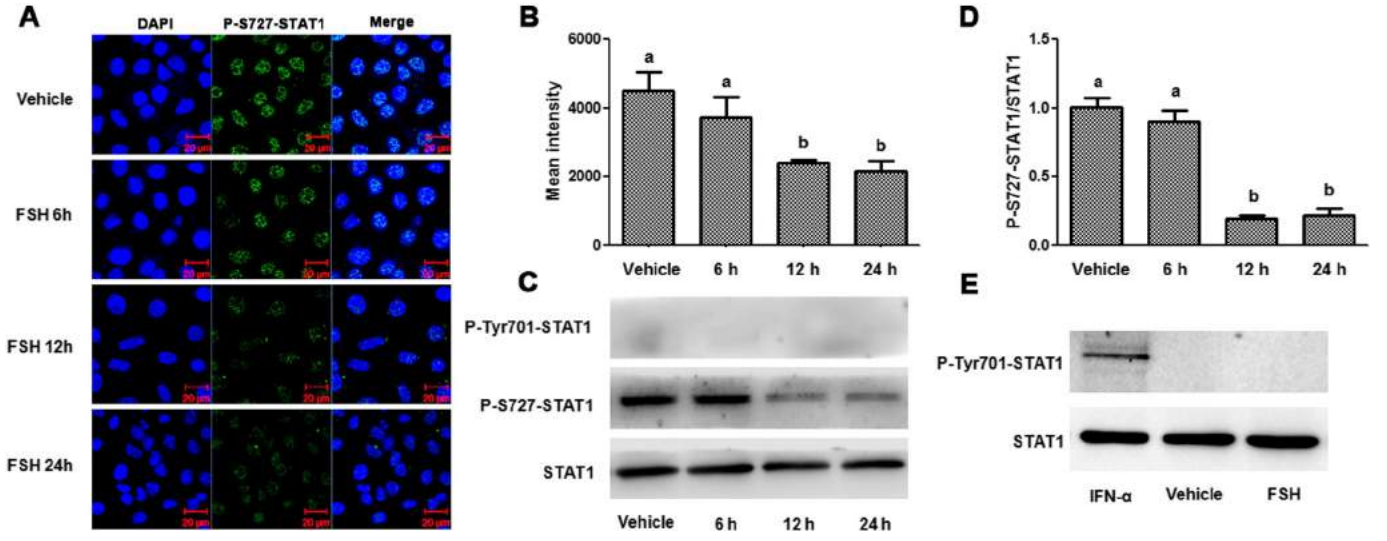

Fig. 9. Effect of FSH on STAT1 TF in cultured granulosa cells of mice *in vitro*. (A) The subcellular localization of p-Ser^{727} STAT1 after FSH treatment was analyzed by immunofluorescence using an anti-p-Ser^{727} STAT1 antibody (green), with the nuclei counterstained with DAPI (blue). Bar = 20 μm. (B) Quantification of p-Ser^{727} STAT1 protein levels by gradation analyses. The ZEN2009 software was used to analyze the gradation presented in panel A. (C) FSH induced dephosphorylation of STAT1 on Ser^{727} *in vitro*. Whole-cell lysates were harvested from the treatment groups as indicated, and immunoblotting was performed to detect p-Tyr^{701}, p-Ser^{727}, STAT1 levels, and STAT1 expression. (D) Quantification of relative STAT1 and p-Ser^{727} STAT1 protein levels by gradation analyses. The ImageJ software was used to analyze the gradation of each band represented in panel C, and the relative expression levels were normalized to that of STAT1. (E) Positive control. p-Tyr^{701} STAT1 in MGCs. Interferon (IFN)-α (500 U/ml) was added to induce phosphorylation of Tyr^{701} on STAT1, and granulosa cell protein was collected after 30 min. Protein samples of the vehicle and FSH groups were collected 24 h after treatment. Graphs show means ± SEM ($n = 3$/group). Letters denote significant ($P < 0.05$) differences between values.

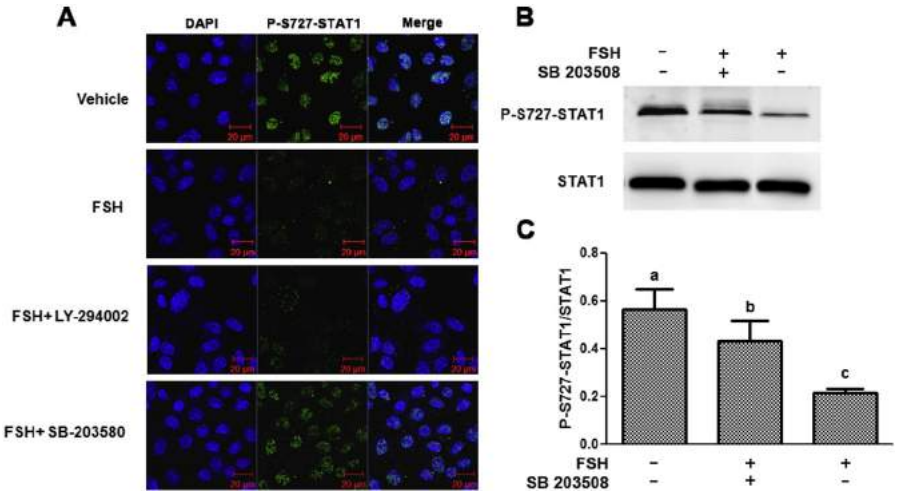

Fig. 10. FSH induction of p-Ser^{727} STAT1 dephosphorylation *via* p38 MAPK. (A) The subcellular localization of p-Ser^{727} STAT1 in cells treated with FSH, LY-294002 and SB203580 was analyzed by immunofluorescence using an anti-p-Ser^{727} STAT1 antibody (green), and nuclei were counterstained with DAPI (blue). Bar = 20 μm. (B) Whole-cell lysates were harvested from the treatment groups as indicated, and immunoblotting was performed to detect p-Ser^{727} STAT1 levels. (C) Quantification of relative p-Ser^{727} STAT1 protein levels by gradation analyses. The ImageJ software was used to analyze the gradation of each band represented in panel B, and the relative expression level was normalized to that of STAT1. Graphs show means ± SEM (n = 3/group). Letters denote significant ($P < 0.05$) differences between values.

polycyclic aromatic hydrocarbons, and halogenated aromatic hydrocarbons such as 2,3,7,8-tetrachlorodibenzo-p-dioxin [33]. FSH and estradiol can reduce AhR protein and transcript levels in rat granulosa cells *in vitro* [34]. AhR can activate the transcription of several target genes, including *Cyp1b1* [35]. Although we hypothesized that STAT1, Pou2f1, NF-E2, and Arnt might function as TFs of *Cyp1b1*, we found that STAT1 is crucial for Cyp1b1 regulation by FSH. The overexpression of STAT1 led to the upregulation of *Cyp1b1* expression. BS 1 and BS 2 were predicted as the binding sites of STAT1 in the *Cyp1b1* promoter region. By mutating the nucleotide sequences in BS 1 and BS 2 (Fig. 7), we determined that the binding sites were functional and played equally important roles in the regulation by STAT1 of *Cyp1b1* transcription activity.

STAT family TFs regulate many aspects of growth, survival, and differentiation in cells. FSH was found to reduce the amount of phosphorylated STAT3, preventing it from binding to DNA in rat granulosa cells [36]. The phosphorylation of STAT1 at Tyr^{701} and Ser^{727} plays a role in regulating gene expression. Whereas phosphorylated STAT1 is translocated to the nucleus to regulate the expression of its target genes, dephosphorylated STAT1 is transported from the nucleus into the cytoplasm, where it loses its regulatory function. The transcriptional activation of Fas and the Fas ligand is dependent on Ser^{727} of STAT1, but independent of Tyr^{701}. Similarly, Ser^{727} but not Tyr^{701} is required for cardiomyocyte death mediated by STAT1 [37]. In breast cancer cells, doxorubicin was shown to activate STAT1 when treated with IFN-γ. Tyr^{701} and Ser^{727} phosphorylation was also enhanced, resulting in increased cell death [38]. Bud-8 normal human fibroblasts treated with IFN-γ showed increased amounts of p-Tyr^{701} STAT1 in their nuclei, with a peak at 20–30 min, stabilization for 2–2.5 h, and disappearance after 4 h [39]. The engagement of the T cell antigen receptor/CD3 complex with Jurkat cells or peripheral blood lymphocytes stimulated the phosphorylation of Ser^{727}, but not Tyr^{701}, of STAT1 [40].

MAPK pathways constitute a large modular network that regulates a variety of physiological processes, such as cell growth, differentiation, and apoptotic cell death. p38 MAPK, a MAPK family member, plays an important role in the phosphorylation and dephosphorylation of some functional proteins [41]. The phosphorylation of STAT1 on Ser^{727} is dependent on the activation of p38 MAPK [42,43]. The Ser^{727} phosphorylation of STAT1 resulted in the highest transcriptional activity [44]. STAT3, constitutively phosphorylated at Tyr^{705} and slightly phosphorylated at Ser^{727} in Vero E6 cells, was dephosphorylated at p-Tyr^{705} by the activation of p38 MAPK [45]. FSH-induced p38 MAPK phosphorylation and activation in rat granulosa cells [46]. In the present study, we found that FSH induced dephosphorylation of p-Ser^{727} STAT1 *via* p38 MAPK (Fig. 10). In MGCs, STAT1 could be phosphorylated at Ser^{727}. p-Ser^{727} STAT1 promoted *Cyp1b1* expression by binding to BS 1 and BS 2 (Fig. 11A), whereas FSH stimulation altered this mechanism. FSH

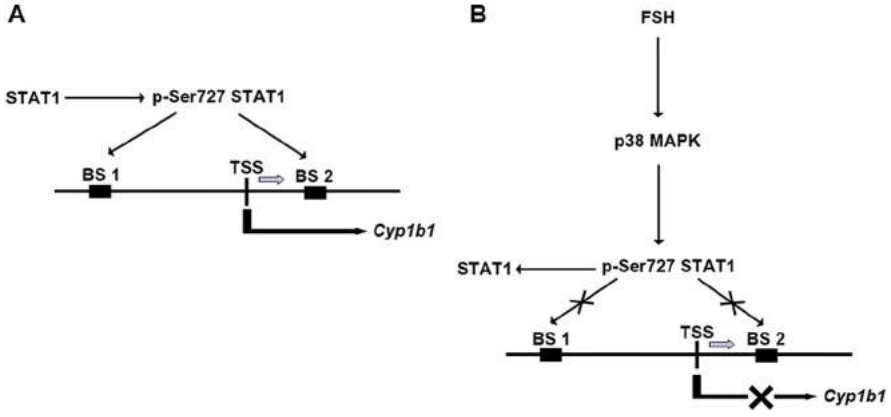

Fig. 11. Model of *Cyp1b1* expression in MGCs. (A) Model of STAT1 regulation of *Cyp1b1* expression. (B) Model of FSH-induced dephosphorylation of p-Ser^{727} STAT1 *via* p38 MAPK, leading to downregulation of *Cyp1b1* expression.

stimulation induced dephosphorylation of p-Ser^{727} STAT1 *via* p38 MAPK in MGCs. Dephosphorylated STAT1 did not bind to BS 1 and BS 2, and lost its ability to regulate *Cyp1b1* expression (Fig. 11B).

5. Conclusions

This study showed that the estradiol metabolism of dominant follicles is regulated predominantly by the *Cyp1b1* gene. STAT1 regulated the expression of *Cyp1b1* through binding to BS 1 and BS 2. FSH induced dephosphorylation of p-Ser^{727} STAT1 activities *via* p38 MAPK, which downregulated *Cyp1b1* expression and maintained estradiol levels in dominant follicles. This mechanism may facilitate the growth of dominant follicles beyond the critical point of atresia and resume meiosis, leading to ovulation.

Acknowledgment

We thank Ming Shen and Kai Xiong for their technical assistance. We thank Ze-Qun Liu and Lie-Chun Li for generously providing the material. The authors declare no conflict of interest. This work was supported by the National Natural Science Foundation of China (31072028) and the key project of the Chinese National Programs for Fundamental Research and Development (973 Program 2014CB138502).

References

[1] S. Kagabu, M. Umezu, Reprod. Med. Biol. 3 (2004) 141–145.
[2] J.E. Fortune, Biol. Reprod. 50 (1994) 225–232.
[3] B. Lunenfeld, V. Insler, Gynecol. Endocrinol. 7 (1993) 285–291.
[4] S.J. Sunderland, M.A. Crowe, M.P. Boland, J.F. Roche, J.J. Ireland, J. Reprod. Fertil. 101 (1994) 547–555.
[5] E.J. Austin, M. Mihm, A.C.O. Evans, P.G. Knight, J.L.H. Ireland, J.J. Ireland, J.F. Roche, Biol. Reprod. 64 (2001) 839–848.
[6] F.P. Guengerich, Chem. Res. Toxicol. 21 (2008) 70–83.
[7] L.A. Suchar, R.L. Chang, R.T. Rosen, J. Lech, A.H. Conney, J. Pharmacol. Exp. Ther. 272 (1995) 197–206.
[8] H.P. Yang, J.G. Bosquet, Q.Z. Li, E.A. Platz, L.A. Brinton, M.E. Sherman, J.V. Lacey, M.M. Gaudet, L.A. Burdette, J.D. Figueroa, J.G. Ciampa, J. Lissowska, B. Peplonska, S.J. Chanock, M. Garcia-Closas, Carcinogenesis 31 (2010) 827–833.
[9] S.J. Campbell, C.J. Henderson, D.C. Anthony, D. Davidson, A.J. Clark, C.R. Wolf, J. Biol. Chem. 280 (2005) 5828–5835.
[10] D.C. Spink, C.L. Hayes, N.R. Young, M. Christou, T.R. Sutter, C.R. Jefcoate, J.F. Gierthy, J. Steroid Biochem. Mol. Biol. 51 (1994) 251–258.
[11] M.H. Heim, J. Recept. Signal Transduct. Res. 19 (1999) 75–120.
[12] M.A. Meraz, J.M. White, K.C.F. Sheehan, E.A. Bach, S.J. Rodig, A.S. Dighe, D.H. Kaplan, J.K. Riley, A.C. Greenlund, D. Campbell, K. CarverMoore, R.N. DuBois, R. Clark, M. Aguet, R.D. Schreiber, Cell 84 (1996) 431–442.
[13] J.E. Durbin, R. Hackenmiller, M.C. Simon, D.E. Levy, Cell 84 (1996) 443–450.
[14] J.N. Ihle, B.A. Witthuhn, F.W. Quelle, K. Yamamoto, W.E. Thierfelder, B. Kreider, O. Silvennoinen, Trends Biochem. Sci. 19 (1994) 222–227.
[15] Z.L. Wen, Z. Zhong, J.E. Darnell, Cell 82 (1995) 241–250.
[16] S. Vanhatupa, D. Ungureanu, M. Paakkunainen, O. Silvennoinen, Biochem. J. 409 (2008) 179–185.
[17] P. Kovarik, D. Stoiber, P.A. Eyers, R. Menghini, A. Neininger, M. Gaestel, P. Cohen, T. Decker, Proc. Natl. Acad. Sci. U. S. A. 96 (1999) 13956–13961.
[18] D.A. Frank, Mol. Med. 5 (1999) 432–456.
[19] Y. Fu, W. Sun, C. Xu, S. Gu, Y. Li, Z. Liu, J. Chen, Anim. Genet. 45 (2014) 373–380.
[20] J.L. Rinn, J.S. Rozowsky, I.J. Laurenzi, P.H. Petersen, K.Y. Zou, W.M. Zhong, M. Gerstein, M. Snyder, Dev. Cell 6 (2004) 791–800.
[21] J.H. Dorrington, J.J. Bendell, S.A. Khan, J. Steroid Biochem. Mol. Biol. 44 (1993) 441–447.
[22] J.S. Richards, J.A. Jonassen, A.I. Rolfes, K. Kersey, L.E. Reichert Jr., Endocrinology 104 (1979) 765–773.
[23] R.C. Burghardt, E. Anderson, Cell Tissue Res. 214 (1981) 181–193.
[24] A.J. Hsueh, H. Billig, A. Tsafriri, Endocr. Rev. 15 (1994) 707–724.
[25] Y.S. Moon, B.K. Tsang, C. Simpson, D.T. Armstrong, J. Clin. Endocrinol. Metab. 47 (1978) 263–267.
[26] N. Manabe, Y. Imai, Y. Kimura, A. Myoumoto, M. Sugimoto, H. Miyamoto, Y. Okamura, M. Fukumoto, J. Reprod. Dev. 42 (1996) 247–253.
[27] Z.H. Chen, H.K. Na, Y.J. Hurh, Y.J. Surh, Toxicol. Appl. Pharmacol. 208 (2005) 46–56.
[28] K. Ollinger, G.D. Buffinton, L. Ernster, E. Cadenas, Chem. Biol. Interact. 73 (1990) 53–76.
[29] A.M. Samuni, E.Y. Chuang, M.C. Krishna, W. Stein, W. DeGraff, A. Russo, J.B. Mitchell, Proc. Natl. Acad. Sci. U. S. A. 100 (2003) 5390–5395.
[30] J.G. Liehr, D. Roy, Free Radic. Biol. Med. 8 (1990) 415–423.
[31] M. Shen, F. Lin, J. Zhang, Y. Tang, W.K. Chen, H. Liu, J. Biol. Chem. 287 (2012) 25727–25740.
[32] M. Tsai-Turton, B.N. Nakamura, U. Luderer, Biol. Reprod. 77 (2007) 442–451.
[33] M.S. Denison, S.R. Nagy, Annu. Rev. Pharmacol. Toxicol. 43 (2003) 309–334.
[34] U.A. Bussmann, J.L. Baranao, Biol. Reprod. 75 (2006) 360–369.
[35] A. Jacob, A.M. Hartz, S. Potin, X. Coumoul, S. Yousif, J.M. Scherrmann, B. Bauer, X. Decleves, Fluids Barriers CNS 8 (2011) 23.
[36] D.L. Russell, J.S. Richards, Mol. Endocrinol. 13 (1999) 2049–2064.
[37] A. Stephanou, T.M. Scarabelli, B.K. Brar, Y. Nakanishi, M. Matsumura, R.A. Knight, D.S. Latchman, J. Biol. Chem. 276 (2001) 28340–28347.
[38] M. Thomas, C.E. Finnegan, K.M.A. Rogers, J.W. Purcell, A. Trimble, P.G. Johnston, M.P. Boland, Cancer Res. 64 (2004) 8357–8364.
[39] R.L. Haspel, M. SalditGeorgieff, J.E. Darnell, EMBO J. 15 (1996) 6262–6268.
[40] A.M. Gamero, A.C. Larner, J. Biol. Chem. 275 (2000) 16574–16578.
[41] M.R. Junttila, S.P. Li, J. Westermarck, FASEB J. 22 (2008) 954–965.
[42] K.C. Goh, S.J. Haque, B.R.G. Williams, EMBO J. 18 (1999) 5601–5608.
[43] D. Stoiber, P. Kovarik, S. Cohney, J.A. Johnston, P. Steinlein, T. Decker, J. Immunol. 163 (1999) 2640–2647.
[44] P. Kovarik, M. Mangold, K. Ramsauer, H. Heidari, R. Steinborn, A. Zotter, D.E. Levy, M. Muller, T. Decker, EMBO J. 20 (2001) 91–100.
[45] T. Mizutani, S. Fukushi, M. Murakami, T. Hirano, M. Saijo, I. Kurane, S. Morikawa, FEBS Lett. 577 (2004) 187–192.
[46] F.Q. Yu, C.S. Han, W. Yang, X. Jin, Z.Y. Hu, X.Y. Liu, J. Endocrinol. 186 (2005) 85–96.